Research Article

Effect of organic and inorganic reinforced particulates for fatigue behaviour of Al–Si7–Mg0.3 hybrid composite: V-notched and un-notched specimen experiments with microstructural constituents

S. Ramanathan[1] · B. Vinod[1] · M. Anandajothi[2]

Abstract
The design of industrial cast parts Al–7Si–0.3Mg alloy is widely used as structural components of aircraft and automotive safety components. The investigation mainly focuses on fatigue life influenced by organic and inorganic particles with different weight fractions measured at different stress levels over a wide range spectrum of three different materials which are evaluated and compared. The notch and un-notch specimens of these materials are described fatigue strength and crack mechanism using high cycle fatigue. According to Basquin constants, fatigue notch factor and notch sensitivity factor were studied. The A356/7.5% rice husk ash-7.5% fly ash hybrid composite increases fatigue strength of 30% and lower the fatigue notch factor to 25% compared to the matrix alloy. Porosity is the main factor for estimation of fatigue life. The micro-/macro-cracks and fracture surface are revealed under the SEM and optical microscope analysis.

Keywords Organic–inorganic · Notch sensitivity factors · Porosity · V-notch and un-notched fatigue strength

1 Introduction

Composite materials are a homogeneous mixture of two or more phases such as matrix and reinforcement which are recognisable between them. The hybrid composites are more potential to replace metal matrix composites due to its enhanced properties. The industry growth and people's life improvement greatly depend on the use of an alternative product in various fields. Hybrid composites consist of organic and inorganic nature in order to yield better stiffness, high strength-to-weight ratio and other mechanical properties [1]. In recent years, the demand for aluminium is increasing day to day for wide applications in the field of industrial sectors, automobile, aerospace, defence, etc. Hence, more intention was made in the development of aluminium-based hybrid composites to explore their possible applications in several high-tech areas. The addition of lightweight reinforcement particles increases more or less continuously with increasing fatigue life values. At present industries mainly focus on hybrid composites replacement of lightweight and reducing material cost. Several agro-waste particles are used as reinforcement like fly ash, jute, bamboo, fibres, rice husk ash. Among various reinforcement, fly ash and rice husk ash (RHA) are achieving more hardness and good resistance to the matrix [2].

In most of the engineering components and machineries, 80% of failures are caused by fatigue. Fatigue process undergoes majorly three stages to identify the fatigue life for structural materials such as fatigue crack initiation, stable-crack propagation and unstable crack propagation. The structures and mechanical components are containing notches and geometrical discontinuities. Generally, the term "notch" is used due to dissimilar in shape for

✉ S. Ramanathan, ramanathan_au@yahoo.co.in | [1]Department of Manufacturing Engineering, Annamalai University, Chidambaram, India. [2]Department of Mechanical Engineering, SNS College of Engineering, Coimbatore, India.

SN Applied Sciences (2019) 1:19 | https://doi.org/10.1007/s42452-018-0015-x

Received: 3 September 2018 / Accepted: 2 October 2018 / Published online: 22 October 2018

several materials. Hence, V-shape threads are widely used as washer's grooves on shafts, non-metallic inclusions corners and fillets [3]. For an aircraft structure in particular rotating parts, notches are needed for their assembly of coupling. The stress concentration is more identified in the notches due to an external force, and also it depends on geometry. However, these stresses are generally higher than that of nominal values. The effect of notches on the behaviour of the material is a challenge to design structure, and moreover, safety is relevant. The formation of a crack at a central point on the notches is usually defined to predict the life of a fatigue. Even for an un-notch specimens for different stress loadings estimation of fatigue life is quite complex. In reuse of waste materials, limited investigations have been performed for such conditions and no generally accepted procedures are exist for performing such analysis. As a result, this is the first attempt to identify the fatigue behaviour for agro-industrial waste materials. The major step is to define fatigue life analysis in between notched and un-notched specimen and also considering fatigue damage for each individual cycle to estimate material life. Moreover, Palmgren [4] was introduced the fatigue damage concept and it was expressed in a linear mathematical form by Miner [5] since to quantify the fatigue failure in different conditions several rules are proposed. Hence, an attempt was made to overcome the fatigue failures using different weight fractions to observe fatigue damage accumulation in experimental studies.

In the present study, the fatigue behaviour of Al A356 alloy and Al alloy with organic (RHA) and inorganic (fly ash) as reinforcement with varying different weight ratios was investigated. The experiment was conducted for both V-notched and un-notched specimens tested at different stress level conditions. Fatigue life analyses are performed using Basquin approach to evaluate material strength, used widely in industrial sectors. The un-notched specimen is studied in order to remove notch effects and improving fatigue life [6]. The results of this investigation are classified in two sections. In the first section, it compares fatigue life estimations to experimental results for notched specimen S–N curve individually, while the same techniques are conducted for an un-notched specimen. In a second section, the combination of all weight fractions along with aluminium alloy similar test conditions is made between the V-notched and un-notched specimens to examine notch and notch sensitivity factor of all compositions. The major part of the current study is focused on a particular region of crack initiation and crack propagation aspects in the estimation of fatigue life, whereas fatigue strength is also analysed using SEM and OM analysis.

2 Experimental procedure and testing methodology

Al A356 alloy with varying wt% of (0, 5 and 7.5) agro- and industrial waste as reinforced particles are fabricated through liquid processing (stir casting) technique. The usage of waste materials is beneficial not only for lower the material cost but also environmental friendly. The fatigue tests are conducted according to Basquin constants for both V-notched and un-notched specimens under different stress levels at constant stress ratio $R = 0.1$ with a frequency of 15 Hz.

2.1 Material selection

Cast aluminium alloys are widely used to manufacture the composite materials which depend upon need in industries. Among other aluminium alloys, A356 alloy consisting of 7% Si, 0.35% Mg and the remaining percentage is aluminium. It has good mechanical characteristics and exhibits high density as well as excellent casting ability, compared to other Al alloys [7]. This material exhibits higher toughness; due to this it is possible to achieve substantial weight reduction and maintaining safety. The chemical composition of aluminium A356 as-received from the company is represented in Table 1.

2.2 Selection of organic and inorganic material

The aluminium hybrid composite materials are generally classified by three major groups such as synthetic ceramic particles, industrial wastes and agro-waste derivate [8]. The waste materials are reused and taken as reinforcement particles to minimise the material cost. In the present work, agro-wastage RHA is taken as first reinforcement due to its high strength-to-weight ratio and lightweight particle. Usage of industrial waste fly ash is taken as secondary reinforcement particle; it provides high resistance to minimise the cost of production. The usage of fly ash as reinforcement not only used in industries but also widely used in construction field attribute to the presence of alumina, and silicon oxide helps to improve material strength. The chemical composition of as-received fly ash and RHA is shown in Tables 2 and 3.

Table 1 Chemical composition of Al A356 alloy

Constituents	Mg	Si	Zn	Mn	Fe	Cu	Others (total)
wt. (%)	0.3	7.0	0.10	0.13	0.15	0.18	Balance

2.3 Fabrication and preparation of hybrid composites

Before casting of hybrid composites, preparation of rice husk into ash was done. At first, rice husk was cleaned with water to eliminate dust particles and dried at room temperature for 24 h. Then washed rice husk was preheated using a muffle furnace at 200 °C temperature for 1 h to eliminate moisture. At this temperature, the colour of husk was changed yellowish into black due to organic matter. After pre-heating the ash was transferred into a tubular furnace at a temperature of 650 °C for 3 h to reduce carbonaceous constituents of the ash. The rice husk ash exhibits a high amount of silica content which tends to increase density and also improves the hardness of material [9]. For the fabrication of aluminium metal matrix composites, different techniques are used among them stir casting is a commercial technique in the preparation of aluminium hybrid composites which are broadly utilised in the manufacturing of structural components. In this study, Al A356 alloy is taken as a matrix component and RHA/Fly ash is taken as reinforcements at various wt% of (0, 7.5, 10 and 12.5) used in the production of hybrid composite materials. A double stir-casting technique is conducted to fabricate the composite materials. The reinforcement particles are preheated initially to reduce dampness at a temperature of 250 °C. After the aluminium matrix is charged directly by argon gas. Hence, it was heated above the liquidus temperature where the alloy is completely melted in a crucible. Then the liquid matrix was cooled at a 600 °C temperature, and preheated reinforcement particles are added with matrix primary stirring which was done manually for 10 min. The second stirring process was performed for 15 min with an operating speed of 400 rpm using an ultrasonic probe at 1200 W input with a frequency of 20.20 kHz to produce homogeneity mixture and reduce porosity level [10]. The main intention in the utilisation of an ultrasonic probe is to minimise porosity level and uniform distribution between matrix and reinforcement in molten metal. After successful fabrication, then the molten liquid was transmitted into 150 mm long and 20 mm diameter of cylindrical die to solidify.

2.4 Measurement of porosity and tensile tests on hybrid composites

The measuring of porosity level and its size distribution of hybrid composites plays a major role in controlling the mechanical properties and also impacts on fatigue strength. The experimental porosity for alloy and hybrid composites was conducted by water absorption test according to the ASTM C 20 standards [11]. The tensile tests are examined to determine the behaviour of hybrid composites according to the ASTM E 8M-04 standard [12]. However, the tensile specimens are prepared with a diameter of 10 mm and length of 120 mm by using 'Instron universal testing machine' withstand while being stretched before necking at cross section to measure tensile strength, yield strength and percentage of elongation and is represented in Table 4. For evaluating porosity (P) all compositions are calculated using Eq. (1).

$$P = \frac{w_{sat} - w_d}{w_{sat} - w_{sus}} \times 100\% \quad (1)$$

where w_{sat} saturated weight, w_d dry weight, w_{sus} Suspended immersed weight.

Table 2 Chemical composition of Fly ash

Constituent	SiO_2	Al_2O_3	K_2O	Fe_2O_3	Na_2O	Loss on ignition (LOI)	others
wt. (%)	58.91	25.53	0.20	4.93	0.32	4.10	6.02

Table 3 Chemical composition of Rice husk ash

Constituent	SiO_2	Al_2O_3	C	CaO	MgO	Fe_2O_3	Loss on ignition (LOI)
wt. (%)	91.08	2.96	1.62	1.23	0.53	0.21	2.20

Table 4 Porosity and tensile strength values of investigated materials

Materials	Porosity (%)	Tensile strength in (MPa)	Yield stress in (MPa)	Percentage elongation (%)
A356 alloy	2.42	132	90	2.51
A356/5% (RHA–fly ash)	2.33	145	112	2.38
A356/7.5% (RHA–fly ash)	2.24	159	126	2.24

2.5 Frame work of fatigue criterion

The rate of growth with cycles can be calculated by using Basquin equation based on fracture toughness of the material. It is important to distinguish between a number of cycles required to short fatigue cracks and is expressed as

$$S^n N = A \tag{2}$$

where S is stress range, N is number of cycles, and n and A are empirical constants.

The stress concentration factor $k_t = \sigma/S$ is evaluated to characterise the notch factor. However, to analyse the notch effects in fatigue k_t concept is utilised. The actual reduction factor at long fatigue life is evaluated at $N_f = 10^4$–10^7 cycles is known as high cycle fatigue (HCF) notch factor, and it is denoted as k_f. While in fatigue, the notch sensitivity is calculated by notch factor (q) expressed as [13]

$$q = \frac{k_f - 1}{k_t - 1} \tag{3}$$

k_t is theoretical stress concentration factor and it is the ratio of maximum stress to nominal stress.

However, the value of 'q' increases results in decreasing sensitivity it indicates no notch effect. The value of notch factor and stress concentration factor were estimated from empirical material constants which are independent of notch radius. The Peterson suggested empirical curves giving either q or α since stress concentration factor is used. It is suitable to formulate such calculations in terms of k_f.

$$q = \frac{1}{1 + {}^{\alpha}/_{\rho}} \tag{4}$$

$$k_f = 1 + q\left(k_t - 1\right) \tag{5}$$

Combining this with above gives k_f directly from α:

$$k_f = 1 + \frac{\left(k_t - 1\right)}{1 + {}^{\alpha}/_{\rho}} \tag{6}$$

where α is taken as 0.51 mm (0.02 in) for aluminium alloys [14]. The notch radius (ρ) is an analysing method which considers specimen at notched and without notched by using the S–N curve with increasing number of cycles. The fatigue lifetime increases and relative crack rate decreased due to a reduction in fatigue notch factor.

2.6 Model geometry and fatigue test details

Fatigue plays a vital role in the industrial sectors over a considerable period to design automotive parts. At present fatigue test is carried out on MTS 100KN servo-hydraulic testing machine; the specimen is taken to be a beam loaded symmetrically at either end such that the specimen is conducted in HCF regime. The diameter (D) of the specimen is 25 mm, and diameter (d) is 75 mm to test section area, more importantly, the ratios of R, D, L and d are maintained at same uniform geometry for all specimens with ASTM E466 norms throughout the experiment [15]. The specimen should greater than two times of the test section and is taken as 120 mm length with inner radius 8 mm. The schematic diagram of a V-notched specimen and un-notched specimen is represented in Fig. 1. The fatigue tests are carried out under high cycle fatigue conditions ($N > 4$), and stress ranges from 80 MPa, 100 MPa and 120 MPa were applied for both alloy and hybrid composites. All the components have been tested at room temperature with a constant amplitude load ratio of $R = 0.1$ and frequency of 15 Hz. Then the specimens are clamped tightly by a collet and also a clamp pressing down type in locking arrangement. Once the machine is started, stress is applied on specimen it acts as a bending moment and thus alternate cycles of the load being imposed on either side of the neutral axis and thereby tensile stress further imposed on mid of the plane. In material testing the crucial thing before testing is inserting material with better loading capability by a pin support otherwise, the specimen will rotate without applying stress. The analysis of macroscopic initiation site is permitted to separate propagation part from initiation part in fatigue test which is an important investigation to conduct experimental results.

2.7 Fractography

To identify the behaviour of a material, optical microscope (OM) is used to capture the fracture appearance of the tested samples. The samples are cleaned with a Kroll's reagent and dried in air to examine the distinct structure of a material. The analyses of microstructural

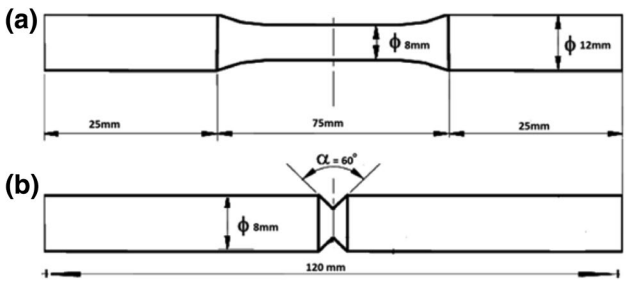

Fig. 1 Dimensions of (**a**) un-notched fatigue specimen and (**b**) V-notched fatigue specimen

studies are conducted using a scanning electron microscope (SEM Model JSM 5610 LV) on fatigue test samples. The elements in each component were identified by phase distribution which was observed by XRD pattern.

3 Results and discussion

The effect of wastage particles as reinforcement with Al A356 alloy was determined using S–N Curve. The fatigue tests were performed for all specimens with a stress level of 80–120 MPa and frequency of 15 Hz at a constant stress ratio of $R = 0.1$. The microstructure evolution of high and low magnification of aluminium alloy and hybrid composites at different stress levels is investigated through SEM.

3.1 Determination of porosity and tensile strength

The porosity plays a crucial role in maintaining the stability of a material and hence it is required to keep porosity low which influences mechanical properties as well as fatigue life [16]. While the addition of reinforcement particles tends to decrease porosity level, for A356/5% RHA–5% fly ash hybrid composite it is identified as 2.33%. The recorded results are evidenced for A356/7.5% (RHA–fly ash); hybrid composite (2.24%) is reduced; open pores are filled by reinforcement particles compared to A356 alloy (2.42%) attributed to poor wettability. However, A356/7.5% RHA–7.5% fly ash hybrid composite has achieved better potential reinforcement for the preparation of hybrid composites. The tensile test was conducted on the polished specimens for alloy hybrid composites. Tests were conducted for two specimens at each composition, and average readings are reported. From Table 4, lower tensile strength is obtained in A356 Al alloy, it is attributed to high agglomeration, and poor wettability is identified in casting. It is observed that addition of weight fraction of reinforcement particles tends to increase tensile strength up to 159 MPa for A356/7.5% RHA–7.5% fly ash hybrid composite and this is because the presence of high amount of silica content not only increases tensile strength but also increases yield stress.

3.2 Microstructure analysis of elemental components

The optical micrographs of Al A356 alloy with agro-industrial waste as reinforcement particles at a different wt% of (0, 5 and 7.5) are shown in Fig. 2. From Fig. 2a, the grain shape of aluminium is larger column; the alloy containing micro-pores which are identified on material surface attributed to more porosity level. In Fig. 2b it is identified that cracks are minimised than that of as-cast alloy; this is due to an addition of hard reinforcement particles. The micro-pores/pits are filled with hard particles and are shown in Fig. 2c. The structure of each element for optical microstructure is investigated by using X-ray diffraction to study phase equilibrium as well as the crystal structure. From XRD pattern, sharp Al phase peaks are exhibited as shown in Fig. 2a. In the case of A356/5% RHA–5% fly ash specimen, Al peaks slightly reduced due to less amount of Al_2O_3 is present, which is shown in Fig. 2b. The intensity of Al phase (peak) decreases while the addition of A356/7.5% RHA–7.5% fly ash subsequently grew up new peaks; this is due to a high amount of SiO_2, Al_2O_3, and Fe_2O_3 as shown in Fig. 2c. This study was concluded that reliability of waste reinforcement particles is thermodynamically stable at elevated temperature and hence plays an important role to form the new brittle phases [11].

The particle size of an inorganic waste particle is taken as 15 µm, whereas organic waste particle is taken as 23 µm which influences the mechanical properties and creates a uniform distribution. The particle size of an as-cast alloy is taken as 32.04 µm and is shown in Fig. 3a. The flakes are identified due to the addition of rice husk ash particles, and spherical shapes are observed attributed to a mixture of fly ash particles which are shown in Fig. 3b, c [17].

3.3 EDS analysis

Typical EDS analysis is carried out on aluminium hybrid composites under different stress conditions at a constant frequency of 15 Hz with a stress ratio of $R = 0.1$. A typical EDX spectrum of Al alloy at a stress level of 100 MPa was identified sharp peaks of Al and Mg as shown in Fig. 4a. The EDS of aluminium alloy shows a low intensity of Si peak, and high intensity of Al peak indicates plastic deformation in alloy during sliding. The new peaks 'O' and 'C' are observed, while the addition of organic and inorganic particles at a stress level of 100 MPa is shown in Fig. 4b. The intensity of Si and Fe peaks indicates the presence of reinforcement particles. Those peaks are increased clearly seen in Fig. 4c; this is due to further increasing RHA–fly ash particles with Al alloy at a stress level of 100 MPa results in improving the toughness of a material. Hence, it is concluded that from the EDS spectrum no oxygen peaks are formed attributed the presence of argon gas was maintained stable throughout fabrication [18]. Therefore, the A356/7.5% RHA–7.5% fly ash hybrid composite is a good choice for automobile sectors.

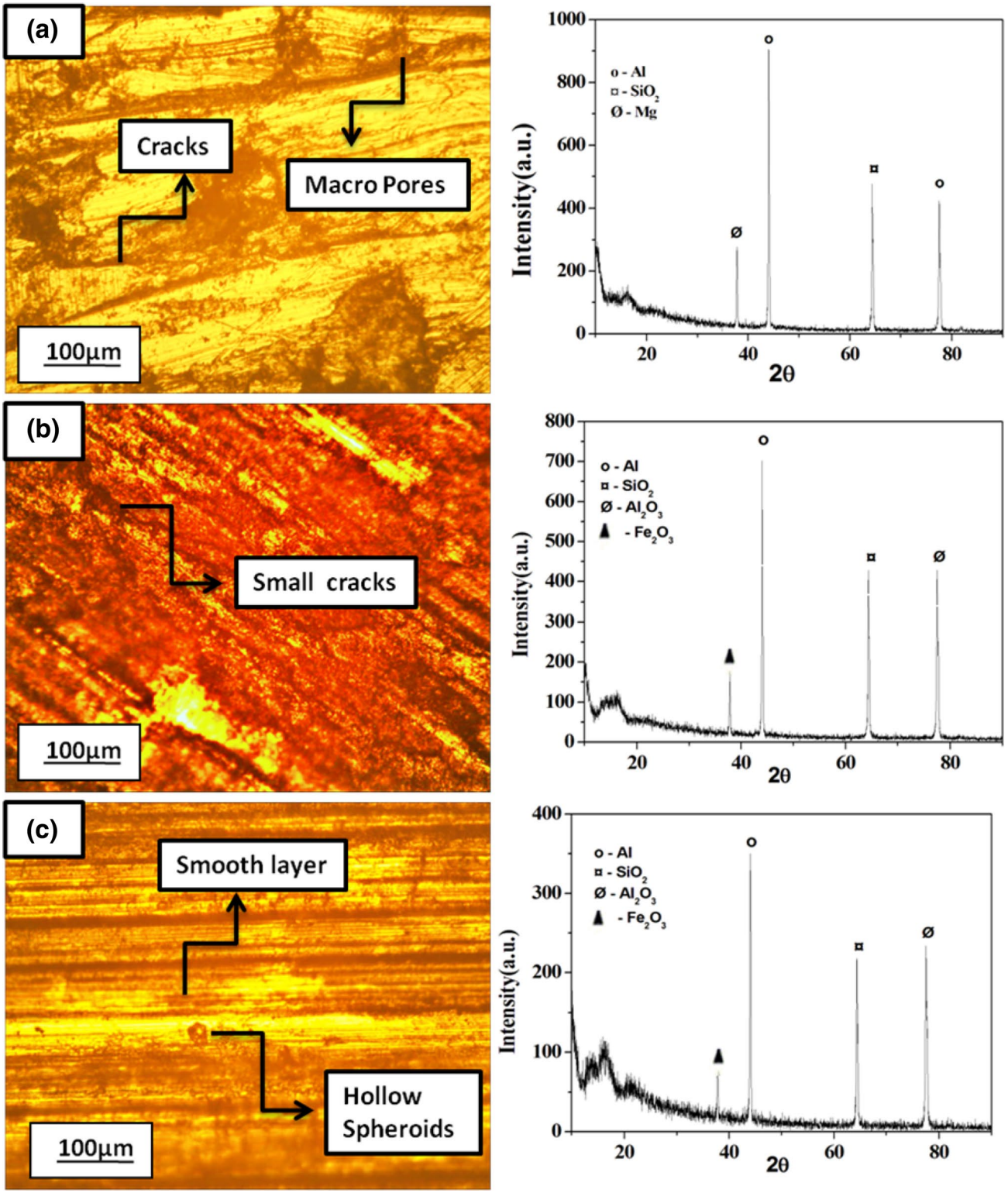

Fig. 2 XRD and Optical micro graphs of (**a**) A356 alloy, (**b**) A356/5% RHA–5% Fly ash and (**c**) A356/7.5%RHA–7.5%Fly ash hybrid composites

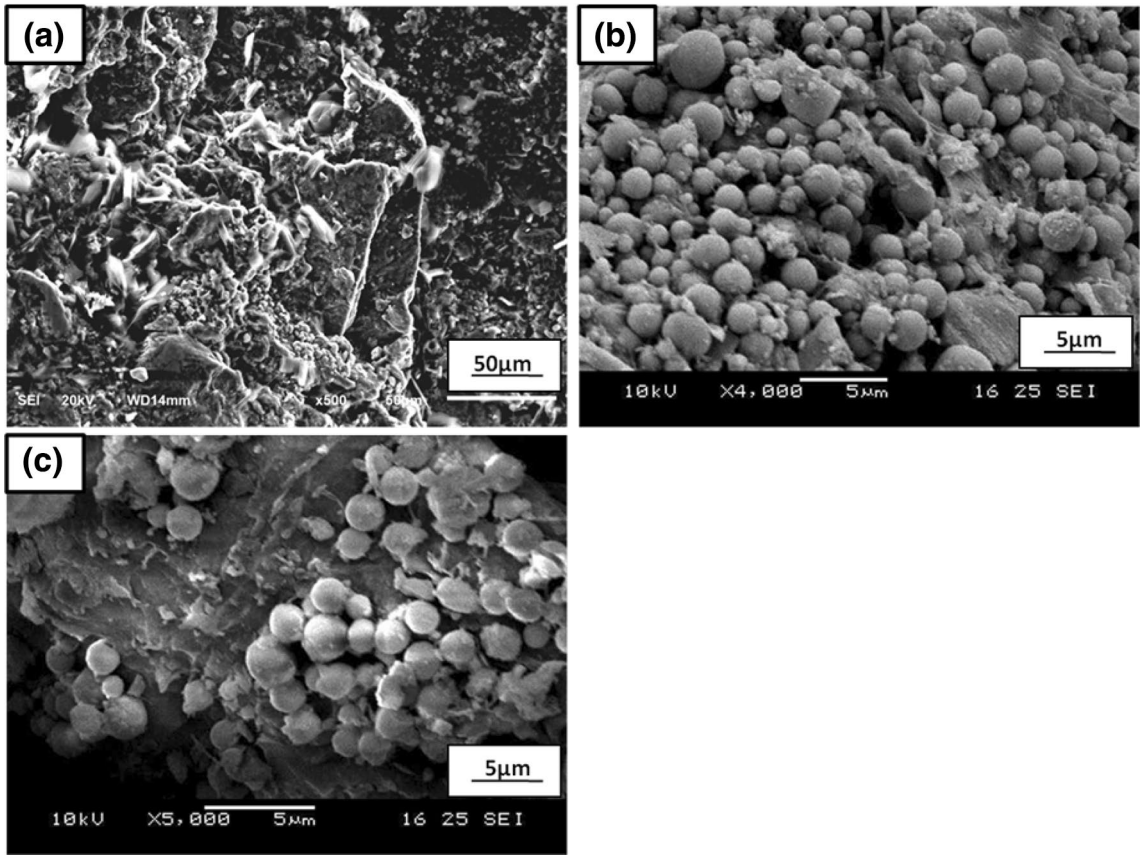

Fig. 3 SEM images of initial microstructure of (**a**) A356 alloy, (**b**) RHA and (**c**) Fly ash particles

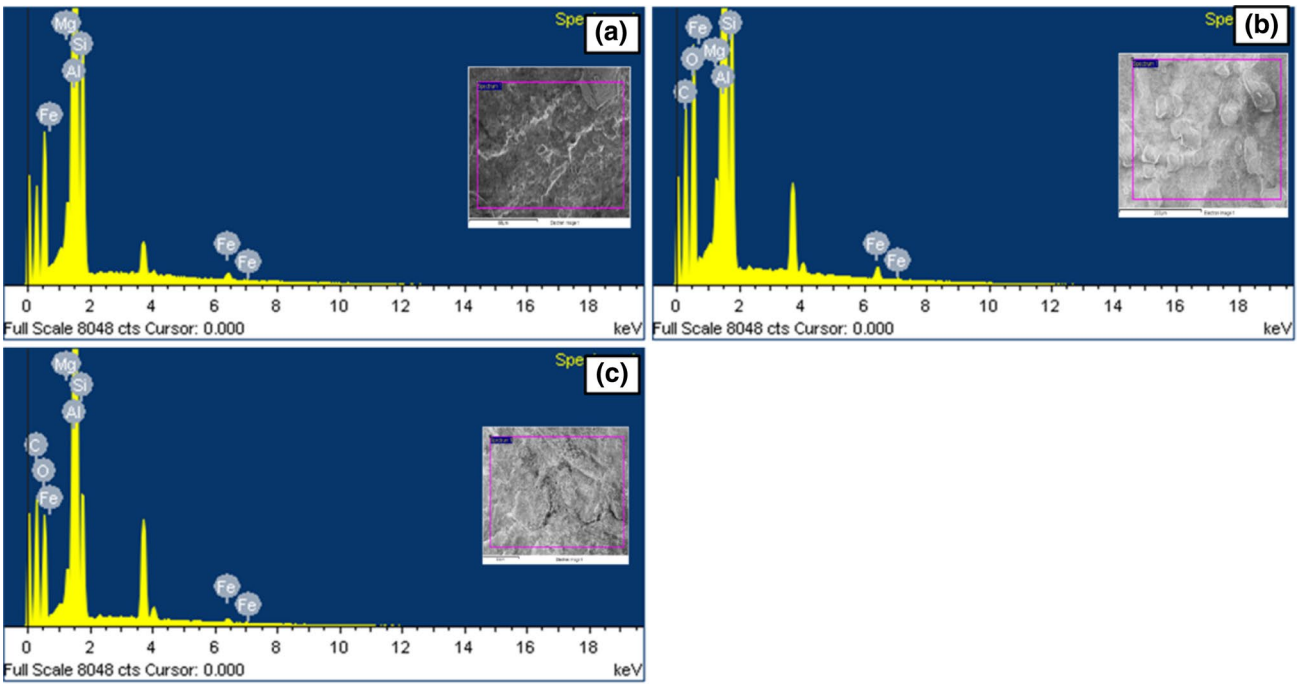

Fig. 4 EDS Analysis of (**a**) A356 Alloy, (**b**) A356/5% RHA–5% fly ash and (**c**) A356/7.5% RHA–7.5% fly ash hybrid Composites

3.4 Stress amplitude calibration on notched and un-notched specimen

The S–N curve is generally to understand the deviation of each material when subjected to cyclic loads. In order to perform fatigue tests efficiently long life regime, this study has been developed a high efficiency of testing machine in respective different stress parameters with axial loading. For each stress level, four specimens are tested for notched and un-notched factor; average of three results is plotted for aluminium alloy and hybrid composites. For each sample quantitative measurements of the fatigue crack were tested at different stress levels ranging from 80, 100 and 120 MPa with a frequency of 15 Hz and stress ratio of $R = 0.1$. The response of cyclic stress amplitude as a function for different weight fractions of a notched and un-notched factor is investigated for as-cast Al alloy, and hybrid composites are shown in Fig. 5. The S–N curve of high cycle fatigue is described by using the above Eq. (2). The effect of fatigue life is determined by comparing S–N curves of aluminium alloy and hybrid composites [19]. The data for HCF are plotted in terms of different stress level based on a net section of the specimen in Fig. 5a–c.

In Fig. 5a seen that, characteristic of S–N curves for notched and un-notched factor the number of cycles (N) is characterised while increasing stress amplitude (σ_f) with respective fracture modes has appeared at different locations. The experimental results of the fatigue tests of A356 aluminium alloy reveal a clear difference between the stress range, and number of cycles is plotted and fatigue limit was observed on aluminium alloy in the investigated region. The S–N curve is determined

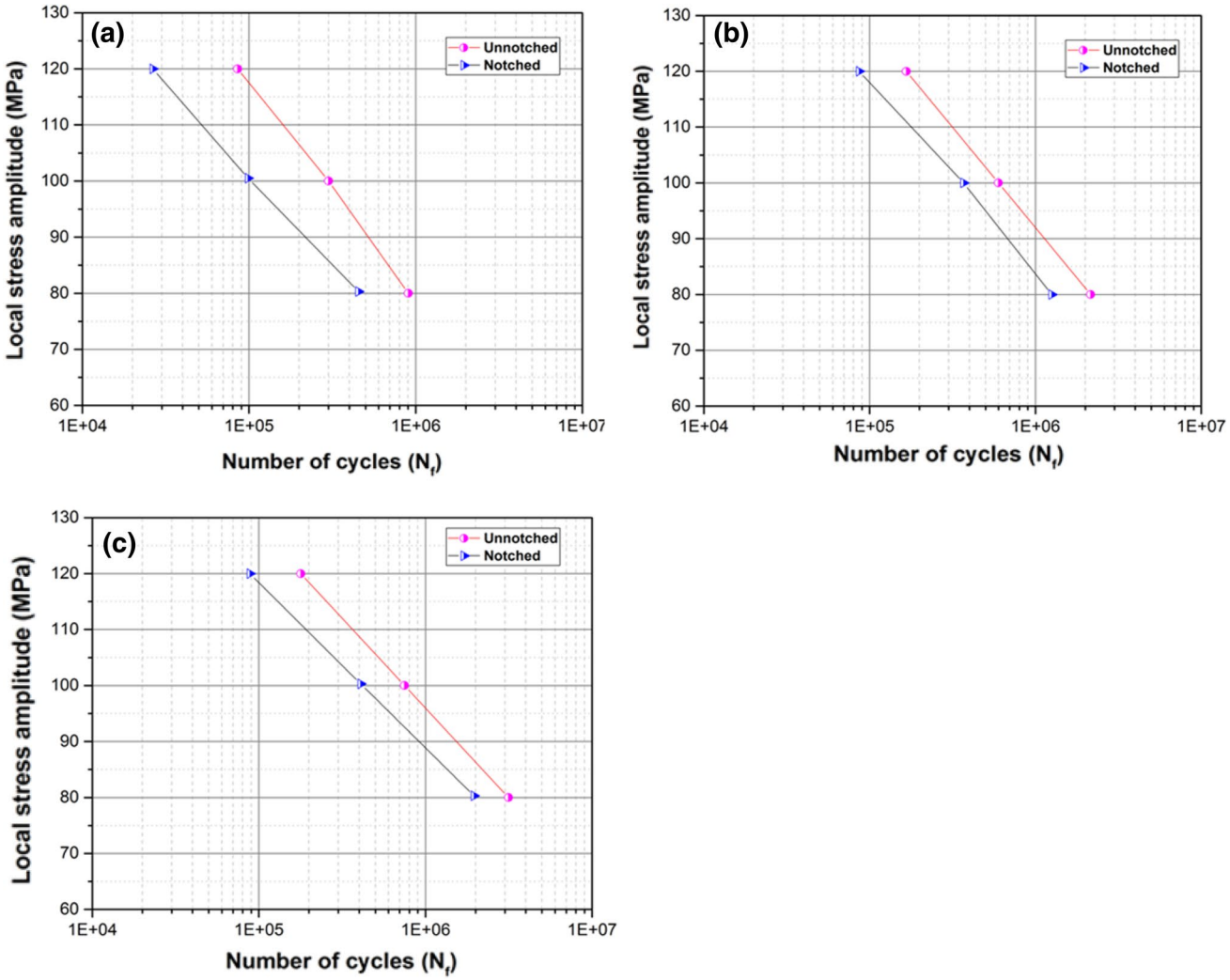

Fig. 5 Comparisons of number of cycles vs estimated stress amplitude for notched specimen and un-notched specimen variable fatigue tests. Estimated lives were computed based on different weight fractions of (**a**) Al A356 alloy, (**b**) A356/5% RHA–5% fly ash hybrid composite and (**c**) A356/7.5% RHA–7.5% fly ash hybrid composite

with a comparison of experimental results. However, the failure started at a higher stress level of 120 MPa, which is attributed due to a low number of cycles initiated. At lower stress level of 80 MPa though the number of cycles is increased still the crack initiated internally. However, other defects could not be found in the un-notched specimen compare to a notched specimen at a minimum stress level of 100 MPa was applied; this kind of fatigue crack is known as a non-defect failure. Hence the stress increased above the threshold limits and fatigue life decreased with increasing number of cycles. The experiment results of the fatigue tests of A356/5% RHA–5% fly ash with different stress conditions are conducted to determine the fatigue life where material tends to brittle fracture. At the stress level of 80–100 MPa region, the number of cycles increases and tends to increase fatigue strength. While increasing the stress up to 120 MPa fatigue lifetime is dropped suddenly 5% of maximal stress before the fracture of the specimen attributes to decrease material stability failure initiated internally and is shown in Fig. 5b; same observations are identified by Sonsino and Franz [20]. Increasing a mixture of lightweight particles to matrix alloy at minimum stress (i.e. 80 MPa), cyclic stress range remained essentially and less failure was identified throughout fatigue life. From the weight fraction of A356/7.5% (RHA–fly ash) hybrid composite, it is clearly seen that the hardening capacity decreased with the addition of reinforcement particles and is shown in Fig. 5c. This mainly attributed to lower porosity and increasing hardness compared to matrix alloy. While increasing the stress level beyond 120 MPa, fracture occurs internally at the beginning and tends to decrease the life-span of fatigue. Hence the effect of stress on fatigue life of hybrid composite materials observed for higher stress loading fatigue crack growth increases.

It is inferred that the aluminium alloy endured less number of cycles than aluminium hybrid composites and above stress level of 80 MPa was exhibited a higher number of cycles. The low number of cycles was observed in aluminium A356 alloy is 4.6×10^{-5} cycles. The addition of 5% and 7% (RHA–fly ash) with A356 alloy obtained a number of cycles which are 5.6×10^{-6} cycles and 7.4×10^{-6}. The A356/7.5% RHA–7.5% fly ash hybrid composite exhibits longer fatigue life in all stress level conditions than that of aluminium alloy. However, it is noticed that the addition of organic and inorganic particles has a no deleterious effect on material strength increased compared to as-cast aluminium induced in preparing of turbine blades and rotors for engine parts. Therefore, the addition of A356/7.5% RHA–7.5% fly ash hybrid composite results in increasing number of cycles and also it exhibits 25% higher strength than that of aluminium alloy and other hybrid composites.

3.5 Estimation of fracture surface on hybrid composites

The fracture surface is examined in order to identify the microscopic initiation sites. Typical fracture surfaces are investigated using an optical microscope at different stress conditions which are shown in Figs. 6, 7 and 8. The fractographic microstructure at the crack initiation sites of Al alloy with hybrid composites is different and will be discussed in the following sections. At higher load, all specimens A356 alloy and hybrid composites are failed from the surface. The crack initiation regime for a higher number of cycles and lower amplitudes is obtained below the surface was about 0.5–4.0 mm. Figure 6 shows typical surface damage with different stress level conditions on aluminium A356 alloy. The crack initiation mode I occurred when initial stress was applied at 80 MPa, in which slip deformation is identified and is shown in Fig. 6a [21]. However, increasing the stress level of 100 MPa (Fig. 6b), failure initiation tends to reduce slightly due to increasing cycles of particular operation fracture decreased. The large amount of deformation caused due to higher stress 120 MPa was

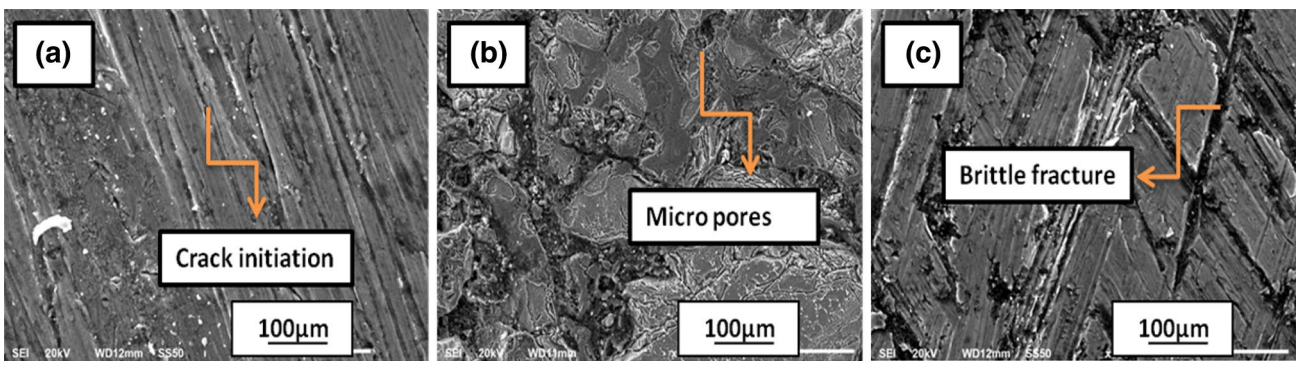

Fig. 6 SEM microstructure of A356 alloy at different strain levels (**a**) 80 MPa, (**b**) 100 MPa and (**c**) 120 MPa

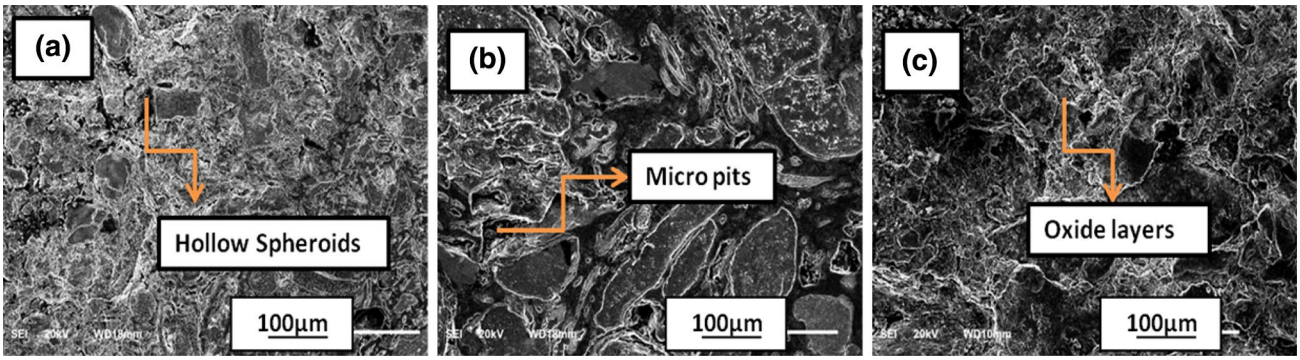

Fig. 7 SEM microstructure of A356/5% RHA–5% fly ash hybrid composite at different strain levels (**a**) 80 MPa, (**b**) 100 MPa and (**c**) 120 MPa

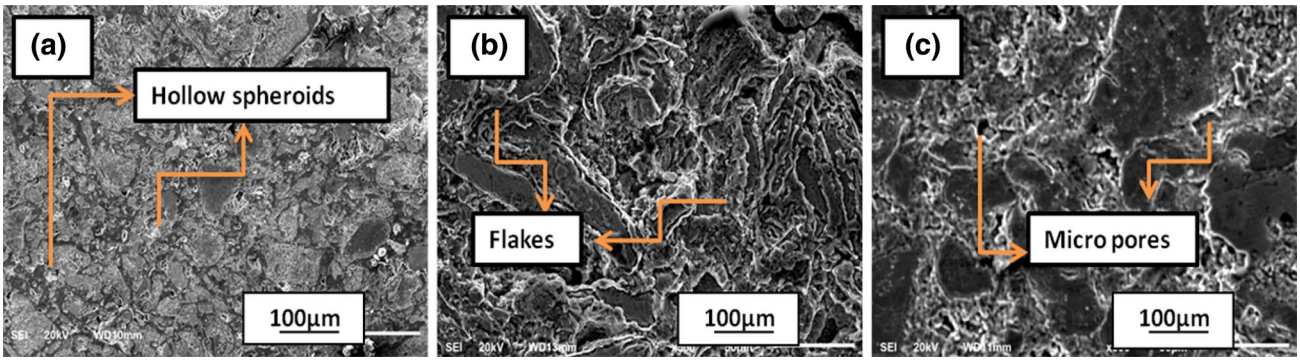

Fig. 8 SEM microstructure of A356/7.5% RHA–7.5% fly ash hybrid composite at different strain levels (**a**) 80 MPa, (**b**) 100 MPa and (**c**) 120 MPa

induced by rubbing it can be seen the brittle fracture on the surface and mode II (secondary cracks) are identified as shown in Fig. 6c. In addition to 5% (RHA–fly ash) with A356 alloy, cracks occurred internally at a lower stress level of 80 MPa as clearly shown in Fig. 7a. When stress level was increased to 100 MPa, it leads to minimise cracks due to the increasing number of cycle's material strength which also increases and small flakes are observed on the material surface as shown in Fig. 7b. Further increase in the stress level at 120 MPa tends to form macro-pores; final failure will occur on 4 mm away from the crack initiation region. This is due to the low toughness, and higher load on material reduces the number of cycles simultaneously; thus, the material tends to severe deformation and is shown in Fig. 7c. Increasing the weight of 7.5% (RHA–fly ash) to Al alloy, homogeneity structure is observed due to the high amount of alumina and silica particles are present on tip of the layer attributed to increasing the material toughness as represented in Fig. 8 [22]. The higher silicon content tends to increase the heat treatment time at room temperature as well as increasing number of cycles. At initial stress 80 MPa small cracks will appear on the surface layer due to lower cycles it reduces mechanical strength as shown in Fig. 8a. The specimens are enhanced by the short crack regime at a stress level of 100 MPa due to higher intensity and lower slip bands which are shown in Fig. 8b. Increasing the stress level of 120 MPa material will deform and tends to fracture on tip of the surface which is shown in Fig. 8c. Therefore, A356/7.5% (RHA–fly ash) hybrid composite is at a stress level of 80–100 MPa; the fracture surface is disappeared and filled by reinforcement particles exhibiting soft mechanism; it results in improving fatigue life. This type of mechanism has increased material strength and preferable for the industrial sector.

3.6 Comparison of stress profiles of notched and un-notched specimen

From the experimental fatigue results, it is identified that 25% of fatigue life is detected due to crack initiation. To find out the crack mechanisms for various stress levels by using a different weight fraction and also to estimate the fatigue life. For the notched and un-notched specimens, fatigue tests are performed based on assumptions of

Basquin theory to identify crack initiation and propagation of composition materials [23]. The result of this analysis is presented in the following sections, including comparisons between experimental and estimated cracking orientations. For all specimens, crack initiation and crack propagation are tested in standard form. From the graphs, it is observed that the aluminium alloy exhibits higher crack growth resistance in all stress level conditions than that of hybrid composites. However, the fracture growth is relatively lower in 7.5% (A356/RHA–fly ash) hybrid composite compare to aluminium alloy. In the notched and un-notched SN curve, at all stress level conditions beyond 100 MPa exhibits lower material strength and reducing fatigue life is observed in this investigation. The fatigue strength of aluminium alloy is achieved as 70 MPa and the fatigue strength of A356/5RHA–5% fly ash and A356/7.5RHA–7.5% fly ash is 84 MPa and 90 MPa which is 25% higher than that of aluminium alloy and other hybrid composites. Hence, the slope of the S–N curve is higher in hybrid composites; it tends to increase the fatigue life. Figure 9 represents increasing stress amplitude as an important function of fatigue life cycle curves in alloys and hybrid composites. As the total stain amplitude increases, fatigue life of the hybrid composites increased as well. In notched and un-notched specimen for A356 alloy is identified lower strength at higher stress level attributes more amount of porosity and low hardness results reduction of material life. It is also noticed that fatigue strength of as-cast Al alloy was sensitive to the fracture modes and significantly reduces the material strength for engineering components due to brittle fracture. The crack growth is minimised while increasing hard particles in Al alloy and is shown in Fig. 9a. However, the definition of failure becomes arbitrary and hence this type of material is not suitable for industrial applications. As noted above, the addition of organic and inorganic reinforcement particles shows a tremendous effect on fatigue strength for both notched and un-notched factors and is shown in Fig. 9a, b. A significant disperse is observed in the tests conducted at 50% of the ultimate tensile strength. The results in Fig. 9b are based on a total failure of the samples which have suggested using 15% stiffness gain compare to notched specimen [24]. In addition of 5% RHA–5% fly ash results in lower stress level with increasing number of cycles, whereas the macroscopic initiation points have been sited results in decreasing fatigue life which is identified at 120 MPa higher stress level. Further addition of 7.5% with Al alloy exhibits a higher number of cycles at a stress level of above 80 MPa due to the presence of high amount of silica content attributes the higher stiffness and increasing material strength as well as fatigue life compared to aluminium alloy. Therefore, from S–N curve it is concluded A356/7.5% RHA–7.5% fly ash hybrid composite content increases toughness and reducing fracture growth rate; it shows life estimation has a larger improvement in both notched and un-notched factor. The un-notched specimen exhibits higher numbers of cycles compared to notched, at a stress level of below 100 MPa, which are beneficial for automobile sectors.

The data of notch factor are plotted in terms of nominal stress. The performance of notch sensitivity is expressed by the fatigue strength reduction factor or fatigue notch factor (k_f) for decreasing the fatigue limit.

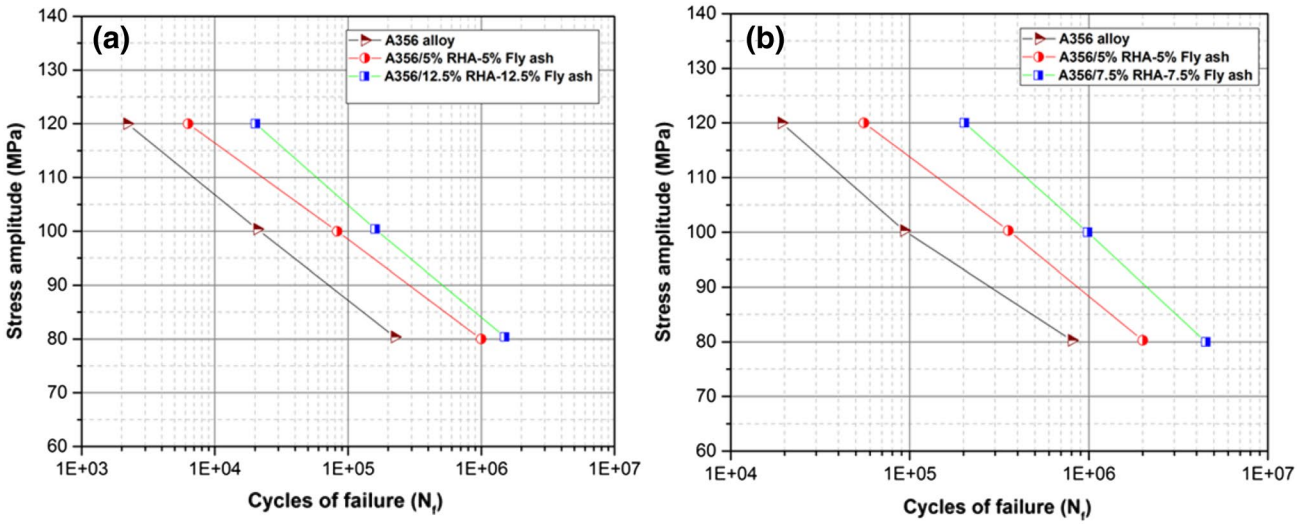

Fig. 9 Comparisons of number of cycles vs estimated stress amplitude for (**a**) notched specimen and (**b**) un-notched specimen variable fatigue tests. Estimated lives were computed based at different weight fractions

Table 5 Fatigue properties of aluminium alloy and hybrid composites

Material	Slope of the S–N curve (*N*)	Intercept of the S–N curve (*A*)	Fatigue strength of the un-notched specimens	Fatigue strength of the V-notched specimens	Notch factor k_f	Notch sensitivity factor (*q*)
A356 alloy	− 0.32	84,560	65	47	1.45	0.280
A356/5% (RHA–fly ash)	− 0.35	89,035	73	54	1.39	0.277
A356/7.5% (RHA–fly ash)	− 0.37	97,132	82	69	1.34	0.261

The fatigue notch factor was conducted, and values are given in Table 5 [25].

$$k_f = \frac{\text{Fatigue strength of the Unnotched specimen}}{\text{Fatigue strength of the notched specimen}}$$

An attempt is made to identify notch factor and notch sensitivity using organic and inorganic materials at different weight fractions. In the literature, no information is available on the effect of notches on fatigue strength of casting metals. The centre cracked tensile specimens are used to evaluate fatigue strength of aluminium alloy and hybrid composites. In calculating the intercept values, 2×10^6 cycles are used for plotting of S–N curve in terms of the corresponding stress range. For this reason in this study, the fatigue strength of aluminium alloy and hybrid composites at 2×10^6 cycles was taken as a basis for comparison to identify the fatigue strength. Hence, it was evaluated for the all hybrid composites as well as aluminium alloy which are presented in Table 5.

The fatigue notch factor of Al A356 alloy, A356/5RHA–5% fly ash and A356/7.5RHA–7.5% fly ash hybrid composite is 1.45, 1.39 and 1.34, respectively, which is lower among the other hybrid composites. However, increasing the fatigue notch factor results in decreasing the fatigue life and hence the aluminium alloy is observed low fatigue strength to notches than the hybrid composites. The fatigue notch factor of the aluminium alloy is 50% higher compared to aluminium hybrid composites. Moreover, the similar trend was observed even in notch sensitivity factor. Therefore, these values are evaluated from fatigue notch factor values and high sensitivity was observed in Al alloy compared to hybrid composites.

3.7 Life estimations based on effect of organic and inorganic particles

The optical micrograph (OM) shows a uniform distribution of the organic and inorganic reinforcement particles in the aluminium matrix. The effect of reinforcement particles was carried out for the notched specimen to identify material strength by using OM investigation. For deeper analysis, high magnification is also taken to identify the cracks on a material surface [26]. The modes of fracture surface have been observed after failure. Figure 10 shows the microstructure of the aluminium alloy primarily promotes low plasticity consists of macropores and fracture on the material surface is due to low density. The fracture surface is increased at higher stress level (i.e. 120 MPa). Three regions are seen in the microstructure of Al alloy such as pre-crack growth, fatigue crack growth and failure regions as shown in Fig. 10a, b. The fracture surface is reduced by the addition of reinforcement particles which is clearly seen in Figs. 11

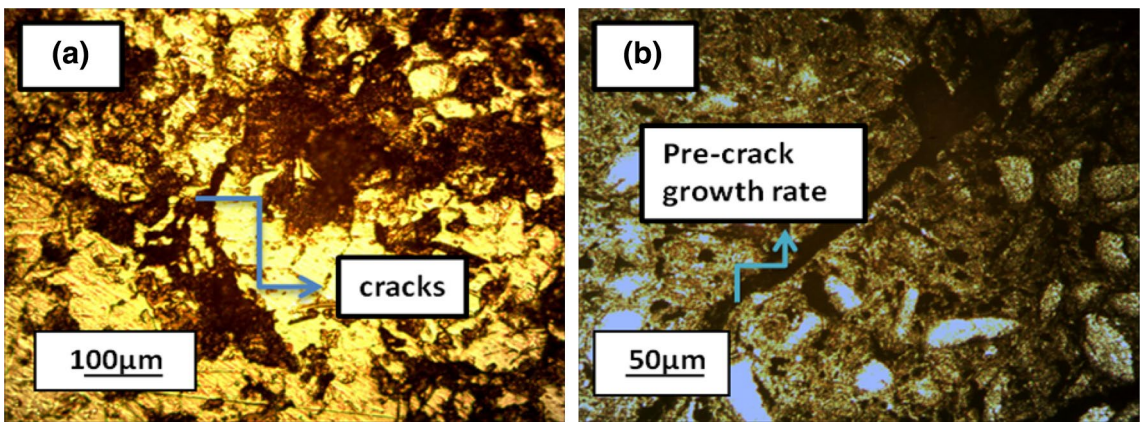

Fig. 10 Effect of Al A356 alloy for notched specimen at (**a**) Low-magnification micrograph and (**b**) high-magnification micrograph

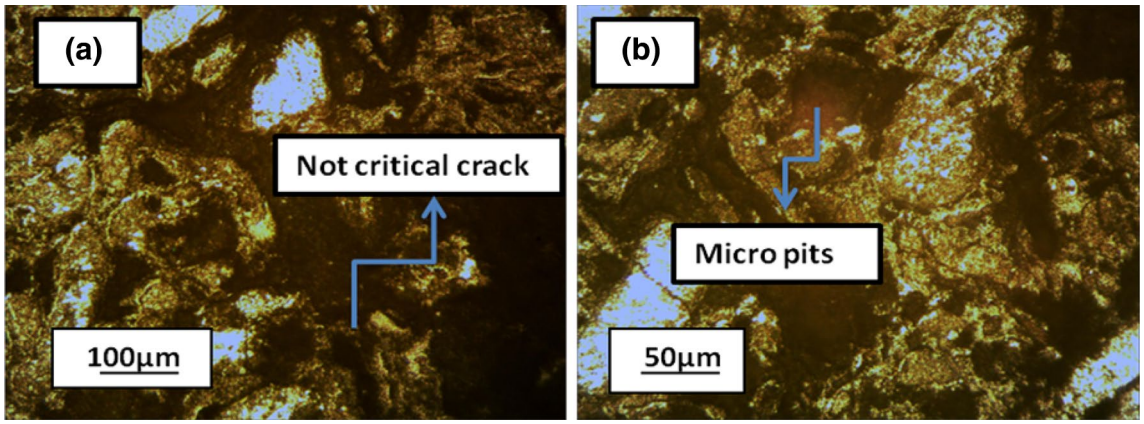

Fig. 11 Effect of organic and inorganic for notched specimen of A356/5% RHA–5% fly ash hybrid composite at (**a**) Low-magnification micrograph and (**b**) high-magnification micrograph

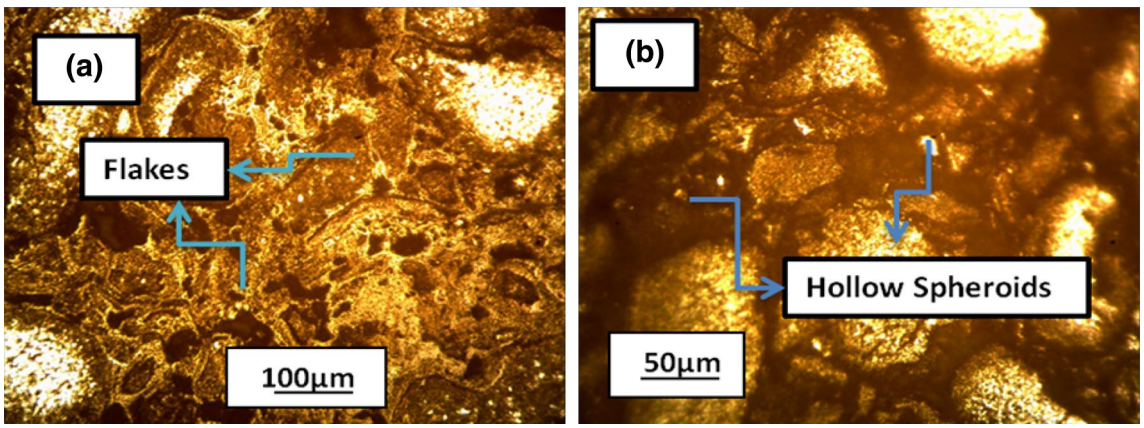

Fig. 12 Effect of organic and inorganic for notched specimen of A356/7.5% RHA–7.5% fly ash hybrid composite at (**a**) Low-magnification micrograph and (**b**) high-magnification micrograph

and 12. A fine second-phase hollow spheroids and small pits are noted by the addition of 7.5% hybrid composite is shown in Fig. 11a. The large dimples are associated at high magnification as shown in Fig. 11b. The microstructure of A356/7.5% (RHA–fly ash) hybrid composite is distinguished easily the shape of pores, cracks disappear and filled by large dimples are in form of Si particles (RHA) and iron-base aluminium oxide (Fly ash) particles and is shown in Fig. 12a, b at a stress level of 120 MPa. The smooth surface is seen due to the high amount of reinforcement particles and helps in increasing the lifespan of material. However, it confirms the effect of porosity level highly influenced by fatigue life on aluminium material.

3.8 Effect of crack orientation comparisons by SEM analysis

Fractography of the un-notched specimen is taken to visualize the fatigue zone, in which the stress is fully reversed, where the irregular striations with random and crack front locations are identically captured using SEM. The fracture modes are assessed and measured using four un-notched specimens under HCF by means of macroscopic as well as microscopic observations. Initially, the samples were etched using a solution composed of 70% of HCl, 29% of HNO_3 and 1% of HF to reveal the grain shapes as shown in Figs. 13, 14 and 15. The fracture mechanism is specified in the following data.

(a) Aluminium A356 alloy Typical microstructure of A356 alloy before the test (Macroscopic) and after the tensile loading (microscopic) crack initiation is observed close to large pores, and cracks is shown in Fig. 13b.

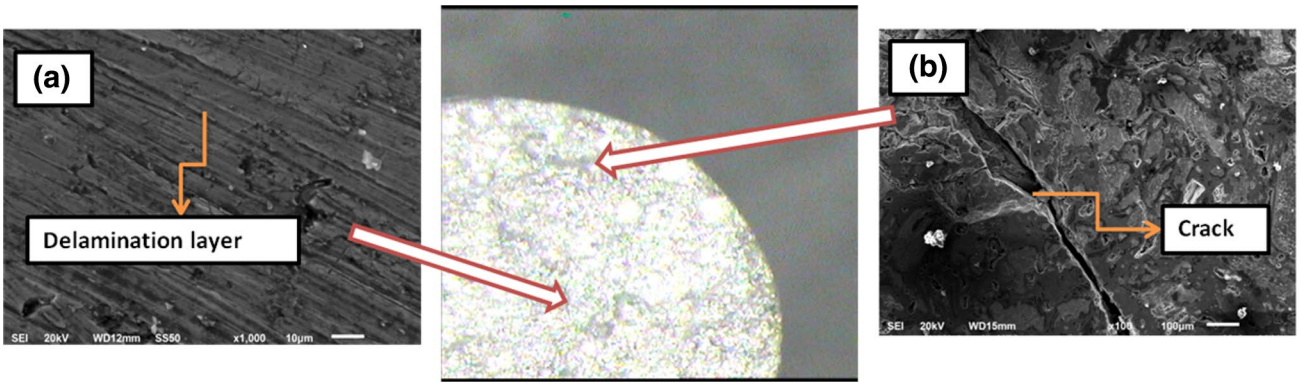

Fig. 13 Typical SEM images of macroscopic and microscopic fatigue fracture surfaces of the un-notched specimen of Al A356 alloy

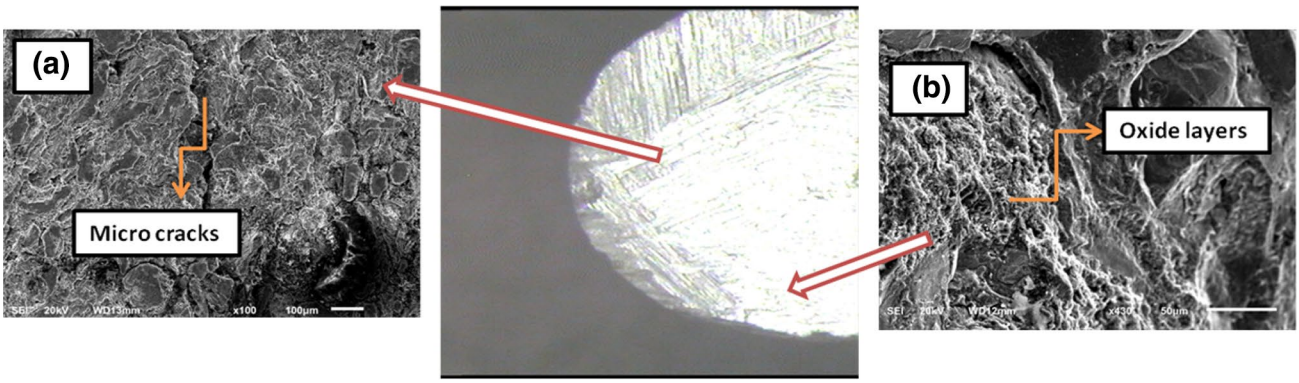

Fig. 14 Typical SEM images of macroscopic and microscopic fatigue fracture surfaces of the slightly un-notched specimen of A356/5% RHA–5% fly ash hybrid composite

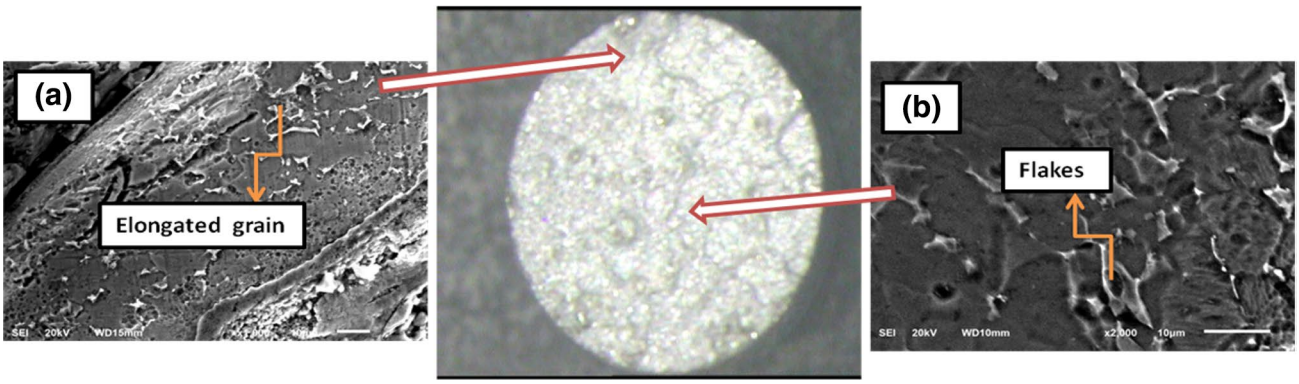

Fig. 15 Typical SEM images of macroscopic and microscopic fatigue fracture surfaces of the slightly un-notched specimen of A356/7.5% RHA–7.5% fly ash hybrid composite

(b) A356/5% (RHA–fly ash) hybrid composite The nucleation of fatigue cracks place along the slip bands (PSBs) acted as crack initiation sites fracture are appeared as shown in Fig. 14. In this case, one sample is not possible to identify crack initiation. Therefore, four samples are conducted to identify the slip bands at each stress level [27]. Majority of grain boundaries are small angles due to a large size of specimens. Slip bands are growing mainly along with grain boundaries, observed in microscopic mode II and are shown in Fig. 14b.

(c) A356/7.5% (RHA–fly ash) hybrid composite The material consists of grains elongated in one direction (like a

shape of hollow periods and flakes) which appears on material surface and is shown in Fig. 15a. The cracks and slip bands are lower due to the addition of reinforcement particles increases to matrix phase which are proved in the SEM image of Fig. 15b. This is due to a high amount of 'Si' and 'Al_2O_3' particles present in the matrix phase tends to increase the lifetime of fatigue as well as high hardness. Preparing this light-weight material is beneficial for reducing the weight of sheet metal in the structure of aircraft.

4 Conclusion

The utilisation of waste particles into raw materials has a lot of attention in recent years due to its low cost and environmental safety. It is quite challenging by using waste materials and come up with the most relevant ones to the task at hand. In fact, reducing the material weight is significantly necessary for designers which are preferable for automobile sectors and results are summarised as follows:

1. The materials are fabricated using double stir-casting process by ultrasonic probe, and fatigue strength is determined.
2. The influence of different weight fractions at various stress level for un-notched specimens exhibits a higher number of cycles compared to notched specimen represented by S–N graphs.
3. The A356/7.5% RHA–7.5% fly ash hybrid composite increases fatigue strength of 30% and lower the fatigue notch factor to 25% compared to the matrix alloy.
4. Porosity is the main factor that influences fatigue behaviour which helps to improve the lifespan of aluminium material. The A356/7.5% (RHA–fly ash) hybrid composite exhibits a low porosity level with higher mechanical strength.
5. In high cycle fatigue regime beyond 100 MPa stress level, it is observed that fatigue crack initiation is occurred due to shear stress. It is corresponding to crack propagation rates applied at 120 MPa stress level.
6. The fracture surface and pores are reduced by addition of organic and inorganic particles examined by using SEM and OM images, whereas phases are identified by XRD and EDS analysis for A356 alloy and A356/RHA–fly ash hybrid composites.
7. The comparison of a notched and un-notched factor for agro-waste reinforced hybrid composite substantially follows a unique curve which suggests that this approach may be universal.

Compliance with ethical standards

Conflict of interest The authors declare that they have no conflict of interest.

References

1. Singh J, Chauhan A (2016) Characterization of hybrid aluminum matrix composites for advanced applications—a review. J Mater Res T 5(2):159–169
2. Subrahmanyam APSVR, Narsaraju G, Rao BS (2015) Effect of rice husk ash and fly ash reinforcements on microstructure and mechanical properties of aluminium alloy (AlSi10Mg) matrix composites. Int J Adv Sci Technol 76:1–8
3. Afaghi-Khatibi A, Ye L, Mai YW (2001) An experimental study of the influence of fibre–matrix interface on fatigue tensile strength of notched composite laminates. Compos Part B Eng 32(4):371–377
4. Palmgren A (1924) Die Lebensdauer von Kugellagern (Durability of ball bearings). ZDVD 68:339
5. Miner MA (1945) Cumulative damage in fatigue. J Appl Mech 12(3):A159–A164
6. Siegfanz S, Giertler A, Michels W, Krupp U (2013) Influence of the microstructure on the fatigue damage behaviour of the aluminium cast alloy AlSi7Mg0.3. Mater Sci Eng A 565:21–26
7. Mo DF, Guo-Qiu H, Zheng-Fei H, Zheng-Yu Z, Cheng-Shu C, Wei-Hua Z (2008) Crack initiation and propagation of cast A356 aluminum alloy under multi-axial cyclic loadings. Int J Fatigue 30(10–11):1843–1850
8. Dwivedi SP, Sharma S, Mishra RK (2015) Microstructure and mechanical behavior of A356/SiC/Fly-ash hybrid composites produced by electromagnetic stir casting. J Braz Soc Mech Sci Eng 37(1):57–67
9. Chandrasekhar S, Pramada PN (2006) Rice husk ash as an adsorbent for methylene blue-effect of ashing temperature. Adsorption 12(1):27
10. Alaneme KK, Akintunde IB, Olubambi PA, Adewale TM (2013) Fabrication characteristics and mechanical behaviour of rice husk ash-Alumina reinforced Al–Mg–Si alloy matrix hybrid composites. J Mater Res T 2(1):60–67
11. Boopathi MM, Arulshri KP, Iyandurai N (2013) Evaluation of mechanical properties of aluminium alloy 2024 reinforced with silicon carbide and fly ash hybrid metal matrix composites. Am J Appl Sci 10:219
12. Ammar HR, Samuel AM, Samuel FH (2008) Effect of casting imperfections on the fatigue life of 319-F and A356-T6 Al–Si casting alloys. Mater Sci Eng A 473(1–2):65–75
13. Paventhan R, Lakshminarayanan PR, Balasubramanian V (2011) Fatigue behaviour of friction welded medium carbon steel and austenitic stainless steel dissimilar joints. Mater Des 32(4):1888–1894
14. Ciavarella M, D'Antuono P, Demelio GP (2017) A simple finding on variable amplitude (Gassner) fatigue SN curves obtained using Miner's rule for unnotched or notched specimen. Eng Fract Mech 176:178–185
15. Verma BB, Atkinson JD, Kumar M (2001) Study of fatigue behaviour of 7475 aluminium alloy. Bull Mater Sci 24(2):231–236
16. Wang QG (2003) Microstructural effects on the tensile and fracture behavior of aluminum casting alloys A356/357. Mater Sci Eng A 34(12):2887–2899
17. Hwang CL, Huynh TP (2015) Effect of alkali-activator and rice husk ash content on strength development of fly ash and residual rice husk ash-based geopolymers. Const Build Mater 101:1–9

18. Shoumkova A, Stoyanova V (2013) SEM-EDX and XRD characterization of zeolite NaA, synthesized from rice husk and aluminium scrap by different procedures for preparation of the initial hydrogel. J Porous Mater 20(1):249–255
19. Smith RA, Miller KJ (1978) Prediction of fatigue regimes in notched components. Int J Mech Sci 20(4):201–206
20. Sonsino CM, Franz R (2017) Multiaxial fatigue assessment for automotive safety components of cast aluminium EN AC-42000 T6 (G-AlSi7Mg0.3 T6) under constant and variable amplitude loading. Int J Fatigue 100:489–501
21. Susmel L, Taylor D (2012) A critical distance/plane method to estimate finite life of notched components under variable amplitude uniaxial/multiaxial fatigue loading. Int J Fatigue 38:7–24
22. Chandra D, Purbolaksono J, Nukman Y, Liew HL, Ramesh S, Hassan MA (2014) Fatigue growth of a surface crack in a V-shaped notched round bar under cyclic tension. J Zhejiang Univ Sci A 15:873–882
23. Berto F, Gallo P, Lazzarin P (2014) High temperature fatigue tests of un-notched and notched specimens made of 40CrMoV13.9 steel. Mater Des 63:609–619
24. Gates NR, Fatemi A (2017) Multiaxial variable amplitude fatigue life analysis using the critical plane approach, Part I: un-notched specimen experiments and life estimations. Int J Fatigue 105:283–295
25. Lazzarin P, Campagnolo A, Berto F (2014) A comparison among some recent energy-and stress-based criteria for the fracture assessment of sharp V-notched components under Mode I loading. Theor Appl Fract Mech 71:21–30
26. Szabó B, Actis R, Rusk D (2016) Predictors of fatigue damage accumulation in the neighborhood of small notches. Int J Fatigue 92:52–60
27. Mittelman B, Yosibash Z (2015) Energy release rate cannot predict crack initiation orientation in domains with a sharp V-notch under mode III loading. Eng Fract Mech 141:230–241